

AN ADAPTIVE PROCEDURE FOR CARRIER PHASE-BASED GPS/GLONASS POSITIONING

Liwen Dai, Chris Rizos and Shaowei Han

School of Surveying & Spatial Information Systems

The University of New South Wales

Sydney, NSW 2052
Australia

Email: liwen@unsw.edu.au

ABSTRACT

GPS/GLONASS pseudo-range and carrier phase observations are affected by errors such as cycle slips, multipath effects, residual atmospheric biases, orbital errors, inter-channel biases and random noise. Due to the presence of these errors, instantaneous (single-epoch) ambiguity resolution using state-of-the-art GPS techniques becomes quite difficult, and even fails if the observations are seriously contaminated. Unfortunately this is not an unlikely event in kinematic positioning applications. In this paper an adaptive procedure based on a real-time stochastic model estimated from the previous residual series, and a multiple outlier detection algorithm based on correlation analysis theory, is proposed. Tests have been carried out using dual-frequency GPS/GLONASS and GPS-only receivers, and single-frequency GPS/GLONASS receivers, over distances ranging up to 10 kilometres. The results indicate that after applying the proposed adaptive procedure the success rates of ambiguity resolution using a single epoch of data can be significantly improved up to 98.3%, and the kinematic positioning accuracy is very high in the case of a large number of redundant satellites.

1 INTRODUCTION

Centimetre accuracy GPS kinematic positioning can, in principle, be achieved in real-time due to the millimetre resolution of the carrier phase observable if the initially unknown ambiguities are resolved to their integer values. In practice, however, reliable and correct ambiguity resolution depends on 'high quality' observations to a large number of satellites. This constrains its use, making it difficult to address positioning applications in areas where the number of visible satellites is limited. The most obvious way to increase the number of tracked satellites is to combine the observations from the GPS and GLONASS systems. On the other hand, significant errors and biases may exist in GPS/GLONASS pseudo-range and carrier phase observations, which are caused by cycle slips, multipath effects, residual atmospheric biases, orbital errors, inter-channel biases and random noise. Because of these errors, instantaneous ambiguity resolution with state-of-the-art GPS techniques becomes quite difficult, and even fails if observations are seriously contaminated, which is a common event in kinematic positioning applications.

For ambiguity resolution and positioning purposes, the minimum number of satellites is 5 for GPS or GLONASS, or 6 for combined GPS and GLONASS processing. If more satellites are tracked, some of these redundant observations can be removed if they are suspected of being contaminated by outliers or biases. There are three scenarios involved in outlier or bias detection in GPS/GLONASS data processing. The first is that if the ambiguity–float solution cannot pass the χ^2 -distribution statistic test, one or more outliers probably exist in the pseudo-range observations. The second is that if ambiguity resolution fails, the carrier phase observations may also contain one or more outliers or biases. The last scenario is that if the ambiguity resolution still fails even after the two abovementioned scenarios are considered, the positioning solution can still be provided using the previous epoch's fixed ambiguities if there are enough satellites being tracked without cycle slips. The cycle slips can be considered as the most significant outliers.

In order to detect and eliminate the effect of outliers on the results, many methods have been proposed in the literature. In general, all these methods can be divided into two categories. One is that the gross errors are considered to have the same variance but different expectation compared with 'normal' observations. The other is that the gross errors are considered to have the same expectation but different variance. In the case of the former, outliers are included in the functional model. Based on some statistics and specification of the criteria associated with a level of significance, the outliers can be located and removed by comparing the estimated value of the statistic with the critical value (see, e.g., Baarda, 1968; Förstner, 1983; Kubik, 1982; Li, 1988). This method was first proposed by Baarda (1968), and has since been applied in many data processing applications. The problem is that the multiple outliers cannot be located directly, especially for the case of highly correlated observations.

In the second class of outlier detection methods, outliers are included in the stochastic model. This means that the 'suspect' observations should have the biggest variance (or smallest weight). After the appropriate weight or variance matrix has been assigned to the corresponding observations, the influence of the outliers on parameter estimation can be mitigated with a few iterations (see, e.g., Zhou et al., 1997; Shi, 1998). Unfortunately the appropriate variance or weight matrix for the observations containing outliers, especially in the case of highly correlated observations, is not easy to determine.

In this paper the results of an investigation of the stochastic model for GPS and GLONASS carrier phase and pseudo-range measurements is reported on, and a multiple outlier detection algorithm based on correlation analysis theory for correlated double-differenced observations is tested. Tests have been carried out in order to demonstrate the efficiency and performance of the proposed test procedures through the case study examples of the dual-frequency GPS/GLONASS and GPS-only receivers, and single-frequency GPS/GLONASS receivers, over distances ranging up to 10 kilometres.

2 MATHEMATICAL MODELLING

High quality results, estimated from the application of least-squares techniques, require the specification of an optimal functional, and associated stochastic model. However, the stochastic model is dependent on the choice of the functional model. Hence, for a different choice of functional model, a different stochastic model may be needed.

2.1 Functional Model

Due to the different frequencies for the different GLONASS satellites, the difference of two receiver clock parameters is not zero, as in the commonly used double-differenced procedure for GPS. To overcome this problem, single-differenced pseudo-range observations are typically introduced (see, e.g., Pratt et al., 1998; Leick, 1998; Zhodzishsky, 1998; Kozlov et al., 1997; Wang, 1998, Han et al., 1999). The double-differenced (DD) GPS pseudo-range observables and the single-differenced (SD) GLONASS pseudo-range observables have been identified as an optimum functional model in integrated GPS and GLONASS positioning (Rapoport, 1997; Wang, 1998). The DD carrier phase observable between receivers can be expressed as (e.g., Leick, 1998):

$$\mathbf{f}_{kl,n}^{pq} = \left(\frac{f_n^p}{c} \mathbf{r}_{kl}^p - \frac{f_n^q}{c} \mathbf{r}_{kl}^q \right) - (f_n^p - f_n^q) \cdot dt_{kl} + N_{kl,n}^{pq} + \mathbf{e}_{kl,n}^{pq} \quad (1)$$

Where the subscripts k and l identify the ground receivers, and superscripts p and q denote the satellites. $\mathbf{f}_{kl,n}^{pq}$ is the DD carrier phase observable expressed in units of cycles, and $n=1,2$ denotes the L1 and L2 frequencies. λ_n^p and f_n^p are the wavelength and frequency respectively. $N_{kl,n}^{pq}$ is the DD integer ambiguity; dt_{kl} is the difference between the two receiver clock biases in seconds; c is the speed of light; and $\mathbf{e}_{kl,n}^{pq}$ is the carrier phase observation noise and any remaining errors.

The following observables are used:

$$\mathbf{P}_{kl,GPS}^{pq} = \mathbf{r}_{kl}^{pq} + \mathbf{e}_{kl}^{pq} \quad (2)$$

$$\mathbf{P}_{kl,GLONASS}^p = \mathbf{r}_{kl}^p + c \cdot dt_{kl} + \mathbf{e}_{kl}^p \quad (3)$$

Where $\mathbf{P}_{kl,GPS}^{pq}$ and $\mathbf{P}_{kl,GLONASS}^p$ are the DD GPS pseudo-range observable and the SD

GLONASS pseudo-range observable respectively.

2.2 Stochastic Model

GPS and GLONASS observations are affected by several kinds of errors and biases. When forming the double-differences, the main biases are caused by multipath effects, residual atmospheric errors, orbital errors, and inter-channel biases. Due to insufficient knowledge concerning these physical phenomena, the above biases cannot be rigorously accounted for through functional modelling. The stochastic model has to therefore account for both the observation noise and the unmodelled residual biases. The well-known elevation-dependent stochastic model is often used, which may be represented as an exponential function or an inverse of the sine of the satellite elevation angle (El-Rabbany, 1994; Jin, 1995). However, constant coefficients can only reflect error characteristics of the GPS receiver rather than the unmodelled residual biases, which most probably are related to the physical environment. An adaptive Kalman filter has been proposed for real-time stochastic modelling for an integrated GPS/GLONASS/INS system (Wang, 1999). Based on the fact that the residual series of least-squares estimation contains sufficient information concerning the observation noise and biases, a more rigorous stochastic model (Han et al., 1999; Dai et al., 2001) is used in this paper:

$$D_i = Q_{V_i} + B_i(B_i^T D_i^{-1} B_i)^{-1} B_i^T \quad (4)$$

Where D_i and Q_{V_i} are the variance-covariance matrices for the measurements and the residuals respectively. B_i is the design matrix. Due to the similarity of the observing environments, the residuals of the observations show a high degree of temporal and spatial correlation, at least in the short term. In other words, the residual series can be considered as a wide-sense stationary process for short periods (a few minutes). The actual variance-covariance matrix of the residuals can then be estimated from the previous residual series V_i , whose ambiguity sets have already been fixed to their correct values, using the following equation:

$$Q_{V_i} = \frac{1}{N} \sum_{k=1}^N V_{i-k} V_{i-k}^T \quad (5)$$

Where N is the width of the moving window. The minimum N should not be less than the number of DD ambiguities. If N is too large, temporal and spatial decorrelation will occur, and the performance will decrease. Testing has shown that the optimal width of the moving window is in the range of 10-30 epochs with 1-second sampling rate. In practical applications, residuals from the ambiguities-fixed solutions need to be used because the float ambiguity values may absorb some unmodelled errors.

In Equation (5), the variance and covariance of the measurements cannot be estimated directly. An iterative procedure becomes necessary. The initial (or default) variance-covariance matrix is determined by using the previous variance-covariance matrix. Based on the previous measurement residuals, the variance-covariance matrix of the measurements can be rigorously estimated in real-time from Equations (1-3). Normally iterating twice is enough. The default stochastic model should be used at the beginning of the data processing, or for a newly risen satellite, or after a long data gap. The

stochastic model in this paper not only reflects the stochastic characteristics of the observation noise, but also the residual biases due to multipath, the atmospheric delays, the inter-channel biases and the orbital error remaining after double-differencing both the carrier phase and pseudo-range observations. With the help of the estimated variance-covariance matrix, the reliability of ambiguity resolution and the accuracy of the kinematic positioning results can be significantly improved.

3 AMBIGUITY RESOLUTION, VALIDATION AND FAULT DETECTION

3.1 Ambiguity Resolution and Validation

Equations (1-3), combining carrier phase and pseudo-range observations, can be used to estimate the real-valued parameter vector that includes receiver coordinates, ambiguities and clock bias, and their variance-covariance matrix. The associated stochastic model is derived from the residual series over the previous epochs using Equations (4-5). In the case of the ambiguity-float solution, estimates \hat{X}_C (coordinates) and \hat{X}_N (real-valued ambiguities) are obtained using the standard least-squares procedure with a posteriori variance vector $\hat{\mathbf{s}}_0^2 = \frac{V^T P V_{Float}}{n-t-m}$, where $V^T P V_{Float}$ is the quadratic form of the residuals.

Reliable results at this step are dependent on the appropriateness of the stochastic model of the observations with respect to the functional model. The following rejection regions should be employed in order to check the fidelity of the stochastic and functional models:

$$V^T P V_{Float} \geq \mathbf{s}_0^2 \cdot \mathbf{x}_{c_{n-t-m}; 1-\alpha/2}^2 \quad (6)$$

$$V^T P V_{Float} \leq \mathbf{s}_0^2 \cdot \mathbf{x}_{c_{n-t-m}; \alpha/2}^2 \quad (7)$$

Where $\mathbf{x}_{c_{n-t-m}; \alpha/2}^2$ and $\mathbf{x}_{c_{n-t-m}; 1-\alpha/2}^2$ are the lower and upper bounds of the $1-\alpha$ confidence interval for the χ^2 -distribution statistic with $n-t-m$ degrees of freedom respectively. This test is used to monitor the pseudo-range observation quality because Ω_{Float} is only dependent on the pseudo-range observations (Han & Rizos, 1997). If the Ω_{Float} is rejected by Equation (6), the outlier detection procedures should be applied because the outliers may exist in the pseudo-range observations, which are caused by multipath or system biases, or the stochastic model does not reflect the actual accuracy of the observations. If the Ω_{Float} is rejected by Equation (7), a check should be made to determine whether there are enough redundant observations, or whether the stochastic model does reflect the actual accuracy of the observation.

The LAMBDA procedure is then implemented to search the integer ambiguity set (Teunissen, 1994; Han & Rizos, 1995). The validation criteria test suggested by Han (1997), and the ratio test, are implemented. If both tests are passed, the ambiguity resolution is assumed to be correct. The quadratic form of the residuals $\Omega_{Fix,k}$ corresponding to the ambiguity-fixed solution should be compatible with \mathbf{s}_0^2 , represented by the condition:

$$\mathbf{s}_0^2 \cdot \mathbf{x}_{c_{n-1};a/2}^2 \leq \Omega_{Fix,k} \leq \mathbf{s}_0^2 \cdot \mathbf{x}_{c_{n-1};1-a/2}^2 \quad (8)$$

where $\mathbf{x}_{c_{n-1};a/2}^2$ and $\mathbf{x}_{c_{n-1};1-a/2}^2$ are the lower and upper bounds of the $1-\alpha$ confidence interval for the χ^2 -distribution statistic with $n-t$ degrees of freedom respectively. If $\Omega_{Fix,k}$ is rejected, the corresponding integer vector will be rejected. In this case, using the outlier detection procedures, a satellite with the outlier should be removed so as to attempt to fix the ambiguities again, or the previous fixed ambiguities (without cycle slips) should be introduced in order to generate reliable positioning results.

3.2 Fault Detection

In order to further ensure that the ambiguity resolution is correct and reliable, additional global information should be used in the case of dual-frequency data. As is well known, the Total Electron Content (TEC) of the path through the ionosphere has a very strong correlation in space and time. The TEC value for the adjacent epoch should therefore be very similar and this information will be considered the basis for a global test. The difference between the double-differenced ionospheric delay on L1 and L2 carrier phase observations of the satellites j and k is defined as $\nabla\Delta TEC$, which can be represented as follows:

$$\nabla\Delta TEC = \mathbf{I}_1^p \mathbf{f}_{kl,1}^p - \mathbf{I}_2^p \mathbf{f}_{kl,2}^p - \mathbf{I}_1^q \mathbf{f}_{kl,1}^q + \mathbf{I}_2^q \mathbf{f}_{kl,2}^q + (\mathbf{I}_1^p - \mathbf{I}_1^q) \cdot N_{kl,1}^q - (\mathbf{I}_2^p - \mathbf{I}_2^q) \cdot N_{kl,2}^q - \mathbf{I}_1^p N_{kl,1}^{pq} + \mathbf{I}_2^p N_{kl,2}^{pq} \quad (9)$$

Where $N_{kl,1}^q$ and $N_{kl,2}^q$ are single-differenced ambiguities for the reference satellite on L1 and L2 respectively. In Equation (9), it is obvious that the GLONASS $\nabla\Delta TEC$ values are biased by the single-differenced ambiguity at the GLONASS reference satellite. If the double-differenced integer ambiguities are resolved correctly, and no cycle slips occur on the single-differenced carrier phase measurement involving the GLONASS reference satellite, the $\nabla\Delta TEC$ sequence should change smoothly. Otherwise, a 'jump' will occur due to wrong ambiguity resolution. The 'jump' can be determined using the difference $dTEC_{kl}^{pq}$, between $\nabla\Delta TEC$ at the current epoch and its value at the previous epoch for whose ambiguities have been correctly fixed. If wrong ambiguity resolution at the current epoch has occurred, and there are no cycle slips at the GLONASS reference satellite, $dTEC_{kl}^{pq}$ can be represented by:

$$dTEC_{kl}^{pq} = -\mathbf{I}_1^p dN_{kl,1}^{pq} + \mathbf{I}_2^p dN_{kl,2}^{pq} \quad (10)$$

Where $dN_{kl,1}^{pq}$ and $dN_{kl,2}^{pq}$ are the magnitudes of the integer biases caused by wrong ambiguity resolution. It should be noted that $dTEC_{kl}^{pq}$ is not affected by cycle slips, except those related to the GLONASS reference satellite. It should also be pointed out that the accuracy of the final ambiguity-fixed solution, the tropospheric delay and the orbit errors have no influence on the accuracy of $dTEC_{kl}^{pq}$. If single-epoch ambiguity resolution is correct at the current epoch and the previous epoch, $dTEC_{kl}^{pq}$ should be very small. Therefore, the criteria:

$$dTEC_{kl}^{pq} < 5.0 \text{ cm} \quad (11)$$

is used for fault detection. However, some special integer bias combinations cannot be identified (Han, 1997). Obviously, if ambiguity resolution is correct and no cycle slips occur at the GLONASS reference satellite, the condition at Equation (11) will be satisfied. The critical value depends on the ionospheric change and the multipath. The magnitude of the ionospheric change between epochs depends on the sampling rate or the length of data gap. The critical value is selected as 5cm for the experiments described in this paper. It should be emphasized that cycle slips at the GLONASS reference satellite have to be considered in the process of fault detection for ambiguity resolution. It can be seen that when a cycle slip occurs on the GLONASS reference satellite, Equation (9) should be modified to:

$$dTEC_{kl}^{pq} = (\mathbf{I}_1^p - \mathbf{I}_1^q) \cdot dN_{kl,1}^q - (\mathbf{I}_2^p - \mathbf{I}_2^q) \cdot dN_{kl,2}^q - \mathbf{I}_1^p dN_{kl,1}^{pq} + \mathbf{I}_2^p dN_{kl,2}^{pq} \quad (12)$$

Where $dN_{kl,1}^q$ and $dN_{kl,2}^q$ are the single-differenced cycle slip values at the GLONASS reference satellite on L1 and L2 respectively. One cycle slip on L1 (or L2) will result in about 1.5mm (or 2.0mm) bias in $dTEC_{kl}^{pq}$ for the worst case. It is clear that small cycle slips have no significant influence on fault detection. It should be emphasized that single-epoch ambiguity resolution is not affected by cycle slips. Before default detection, a two-step procedure has been suggested in order to check for cycle slips affecting the GLONASS reference satellite. The first step is that after the best ambiguities pass the validation criteria, the GLONASS satellite without significant cycle slips will be selected as the reference satellite. In this step, the difference in the single-differenced TEC with ambiguities between two epochs can be used to detect cycle slips. In practice, significant cycle slips are easily detected. The second step, if the GLONASS reference satellite has been changed, is that the corresponding double-differenced ambiguities will have to be reconstructed. If all the GLONASS satellites are suspected of having significant cycle slips, all the GLONASS observations will be deleted, and the fault detection procedure will not be applied to the GLONASS ambiguities. It should be pointed out that the cycle slips on the single-differenced carrier phase measurement involving the GPS reference satellite have no influence on fault detection. Any ambiguities which cannot satisfy Equation (11) should be rejected. In practice, the suggested fault detection procedure can effectively identify incorrect ambiguity resolution.

4 ADAPTIVE PROCEDURE

Based on the above analysis, adaptation procedures for the functional model can be applied if the Equations (6-7) are accepted, or the Equations (8-9) are rejected. If the resolved integer ambiguities are incorrect, in general the wrong integer ambiguities will refer to more than one satellite pair, and it is almost impossible to identify which ambiguities are incorrect. However, the fact that some significant biases are present in the observations can be confirmed. For ambiguity resolution and positioning purposes the minimum number of satellites is 5 for GPS or GLONASS, and 6 for combined GPS and GLONASS processing. If more satellites are tracked, some of these observations, which are suspected as being contaminated by outliers or biases, can be removed so that: (1) instantaneous ambiguity resolution is possible with a maximum success rate; and (2)

the position solution can still be output using the fixed ambiguities from the previous epoch (if ambiguity resolution fails and there are enough satellites without cycle slips). The objective of the adaptive procedure for the functional model based on the outlier detection algorithm is: (1) to judge whether any outlier is present; (2) to determine which observations should be identified as containing outliers; and (3) to make an acceptable decision about outliers and to estimate the corresponding effect on the final solution if outliers cannot be uniquely identified. All the above are important for a successful outlier detection algorithm. However, the emphasis of this paper will be on the former two issues. In this paper, two outlier detection algorithms are tested.

4.1 Outlier Detection Methods

Baarda's data snooping theory assumes that only one outlier is present in the observations (Baarda, 1968). Applying a series of one-dimensional tests, that is, testing consecutively all residuals, is the standard data snooping strategy. Baarda's Test belongs to the group of un-studentized tests that assume that the a priori variance of unit weight is known. The test statistic is written as:

$$n_i = \frac{V_i}{d_0 Q_{vv_{ii}}} \in N(0, 1) \quad (13)$$

The critical value can be determined from the normal distribution with a significance level of α . If α is assigned 5%, the critical value is 1.96. It can be seen that the critical value for this test is independent of the degrees of freedom.

Outlier Detection Based on Correlation Analysis

Any observation errors, including outliers, affect the residuals through the reliability matrix in the least-squares adjustment. The correlation coefficient between column vector of the reliability matrix and residual vector is considered critical information, which can reflect the relationship between the true error of the correlated observations and the residuals. It replaces the standardized residual for the detection and analysis of the outliers in the correlated double-differenced observations. Therefore, an outlier detection algorithm based on correlation analysis theory was proposed (Shi, 1998; Dai et al., 1999):

$$\mathbf{r}_{R_j, V} = \frac{\sum_{i=1}^n (r_{ij} - \bar{r}_j)(v_i - \bar{v})}{\sqrt{\sum_{i=1}^n (r_{ij} - \bar{r}_j)^2 \sum_{i=1}^n (v_i - \bar{v})^2}} \quad (14)$$

Where r_{ij} denotes the elements in the reliability matrix R . \bar{v} and \bar{r}_j are the average values of the residual vector V and column vector (R_j) related to R matrix respectively. According to the correlation analysis theory, the following statistic for the correlation coefficient test can be obtained (Shi, 1998):

$$\mathbf{r}_{R_j, V} = \frac{t_c}{\sqrt{t_c^2 + n - 2}} \quad (15)$$

Where t_c is the critical value associated with the t-distribution, with a given significant level and $n-2$ degrees of freedom. If the correlation coefficient is greater than the given critical value, it is significant. It indicates the possibility that the observation(s) relating to the significant correlation coefficient(s) should be considered as having been contaminated by outliers. An observation with the largest correlation coefficient should be removed at each iteration. Hence, multiple outliers can be located through an iterative procedure. After the outliers have been located, the outliers should be substituted back into the observations to test them one by one, so that any mis-flagged outliers can be restored.

4.2 Adaptive Procedure

The adaptive procedure (including real-time stochastic model estimation from the previous residual series, and multiple outlier detection algorithm based on correlation analysis theory) for GPS/GLONASS instantaneous ambiguity resolution and positioning can be summarized as follows:

- (1) After computing the ambiguity-float solution using the estimated stochastic model from the residuals, test whether the $V^T P V_{Float}$ is less than a detection threshold defined by the a priori \mathbf{S}_0^2 with degree of freedom $n-t-m$ and significant level $1-\alpha$. If the test is accepted, go to the next step, otherwise go to (3). It should be emphasized that if there are less than the necessary number of satellites when some satellites are removed, go to step (4).
- (2) Attempt ambiguity resolution, and apply validation and fault detection procedures. If one ambiguity set can pass all the tests, output the ambiguity-fixed solution, keep the corresponding residuals and go to step (1) to process the next epoch of data.
- (3) After computing the correlation coefficients between the residuals and the column vectors of the reliability matrix, test whether the maximum correlation coefficient is greater than a detection threshold with degrees of freedom $n-2$ and significant level $1-\alpha$. If true, delete the satellite relating to the maximum correlation coefficient and go to step (1). Otherwise, go to step (4).
- (4) After introducing the previous fixed ambiguity set and restoring all the deleted satellites, test according to Equation (10) using only carrier phase observations. If the test passes, the positioning solution is output. Otherwise, an iterative process, with the satellite relating to the maximum correlation coefficient removed, would be repeated until the test passes, or less than the necessary double-differenced carrier phase observables can be formed. If less than the necessary number of DD carrier phase observables can be formed, the process will be repeated again after some eliminated satellites are restored and the reference satellite is deleted. If all the adaptive procedures still fail, the adaptive procedure is considered to have finally failed. Following this, go to step (1) to process the next epoch of data.

It should be emphasised that if the previous ambiguities, fixed to the wrong values, are introduced in step (4), the wrong ambiguities can easily pass the test according to Equation (10). It will lead to seriously wrong positioning solutions. Hence care should be taken to ensure that the introduced ambiguity sets are indeed the correct ones. In this paper, if the ratio value for the ambiguity validation is greater than 3, the ambiguities can only be introduced in the next epoch. If the outliers, such as cycle slips, exist in the observations, it is almost impossible to pass the test in Equation (10). On the other hand, in order to obtain a precise positioning solution, the satellite geometry should satisfy at least the given conditions ($PDOP < 5$, in this paper).

5 EXPERIMENTS

The proposed adaptive procedure was tested using data from two sets of experiments, involving dual-frequency GPS/GLONASS and GPS-only receivers, and single-frequency GPS/GLONASS receivers.

5.1 Static Experiments

The first is a set of static experiments using data with one-second sampling rate from the dual-frequency GPS/GLONASS JPS receivers and single-frequency GPS/GLONASS Ashtech GG24 receivers. The reference GG24 receiver was set up on the Mather Pillar, on the roof of the Geography and Surveying building, at The University of New South Wales. The user GG24 receiver was set up at different sites, which included the same roof nearby to the reference receiver, at Coogee Beach, at Maroubra Beach, and at the La Perouse Beach. The baseline name, baseline length, number of satellites, observation span (total number of epochs) are given in Table 1. The positioning results can be easily checked from the repeatability of the baseline vectors for the different sessions. In the case of all the data sets the cut-off elevation angle was set to 15 degrees during the processing.

All static baselines were processed in single-epoch mode. Data processing has been carried out for all the static data using two different strategies. One strategy only applies the empirical stochastic model based on the satellite elevation angle, and the other one applies the proposed adaptive procedure.

Table 1. Details of the static test data sets.

Name	Length (m)	GPS/GLN satellites	Total Epochs	Receivers	Survey Date
A1	12	8-5/7-3	14362	GG24	12.5.99
A2	2873	9-5/7-4	4012	GG24	11.5.99
A3	4053	9-6/5-3	6868	GG24	10.5.99
A4	12103	7-5/6-3	9344	JPS	11.08.99

The results are listed in columns 3-5 in Tables 2 and 3. The third column is the number (and percentage) of epochs for which ambiguity resolution is successful on an epoch-by-epoch basis. The fourth column is the number of epochs (and percentage) which do not

pass the validation criteria test. The fifth column is the number of epochs (and percentage) which pass the validation criteria tests, but for which the result is incorrect. In Table 3 there are three sub-columns in column 3, where the first sub-column stands for the total success rate. Case 1 means the ambiguities can be successfully resolved directly; and Case 2 means that the ambiguities can be resolved successfully or whose correct positioning results can be output after the outlier detection algorithm is applied.

Table 2. Single-epoch solution using the elevation-dependent empirical stochastic model.

Name	Total Epochs	Correct (%)	Reject (%)	Wrong (%)
A1	14362	11689(81.4%)	2639(18.4%)	33(0.2%)
A2	4012	3335(83.1%)	677(16.9%)	0(0.0%)
A3	6868	5723(83.3%)	1145(16.7%)	0(0.0%)
A4	9344	9344(100.0%)	0(0.0%)	0(0.0%)

Table 3. Single-epoch solution using the proposed multiple outlier detection algorithm and the real-time stochastic model.

Name	Total Epochs	Correct (%)			Reject (%)	Wrong (%)
		Total	Case 1	Case 2		
A1	14362	14362 (100.0%)	13273 (92.4%)	1089 (7.6%)	0 (0.0%)	0 (0.0%)
A2	4012	4012 (100.0%)	3922 (97.8%)	90 (2.2%)	0 (0.0%)	0 (0.0%)
A3	6868	6821 (99.3%)	6474 (94.3%)	347 (5.1%)	47 (0.7%)	0 (0.0%)
A4	9344	9344 (100.0%)	9344 (100.0%)	0 (0.0%)	0 (0.0%)	0 (0.0%)

It can be seen that using the elevation-dependent empirical stochastic model the success rates for ambiguity resolution range from 81.4% to 100.0%. It should be emphasised that because of the redundant observations and precise pseudo-range data, the ambiguities for the dual-frequency GPS/GLONASS data from the JPS receivers can be fixed easily to the correct ones in the single-epoch mode even though the baseline length is over 10km. It also shows that quite a large percentage of the epochs (0.2%) at baseline A1 give the wrong ambiguity resolution results. After applying the multiple outlier detection procedure and the real-time stochastic model estimated using the residuals from the previous epochs (in this case 10 epochs), the success rates of ambiguity resolution range from 99.3% to 100.0%. No wrong ambiguity resolution results or incorrect positioning results, estimated using fixed ambiguities that are introduced from the previous epoch, are accepted. It is also noted that the multiple outlier detection procedure is responsible for quite a large percentage of epochs (7.6% for A1, 2.2% for A2, 5.1% for A3) whose ambiguities are recovered correctly or whose positioning results are output correctly. The results indicate that single-epoch ambiguity resolution can achieve up to 99.3% success rate with redundant GPS and GLONASS satellite observations. The conclusion that can be drawn is that the multiple outlier

detection algorithm based on correlation analysis theory and the estimated stochastic model from the residuals are, in theory, rigorous and, in practice, very powerful.

The TEC test, which makes use of the correlation information between neighbouring epochs, has been applied in data set A4 for further testing of the ambiguity resolution results. The TEC value should not change by very much within a short time span. This test is a necessary condition, but not a sufficient condition. If the ambiguity resolution cannot pass this test, the ambiguity resolution will also be considered wrong. Figures 1 and 2 show the double-differenced TEC and the corresponding change in the final positioning solutions for GPS and GLONASS satellites respectively. It can be seen from Figure 2 that the GLONASS TEC value has been biased by the single-differenced ambiguity involving the GLONASS reference satellite. However, it will have no influence on the TEC change if no cycle slip occurs on the GLONASS reference satellite.

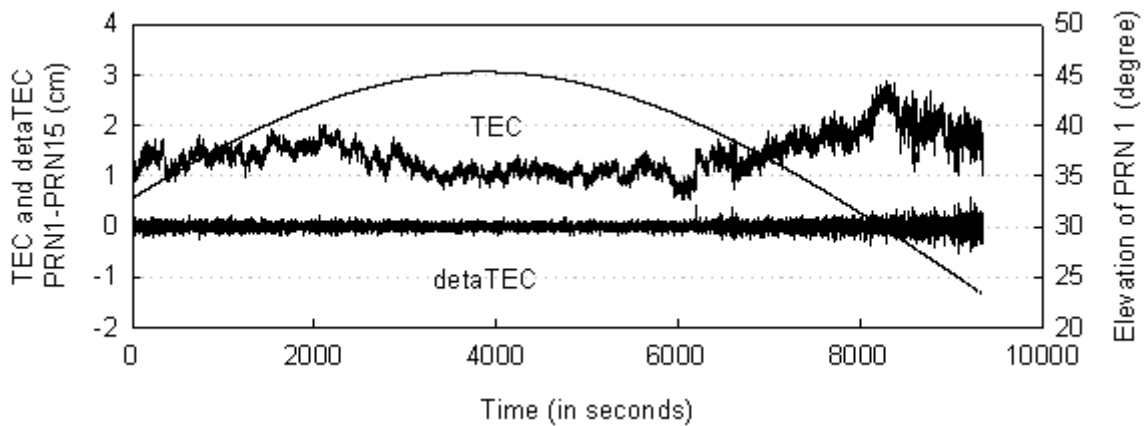


Figure 1. $\nabla\Delta TEC$ and $dTEC$ values for GPS sat 1 (reference GPS satellite 15, with highest elevation).

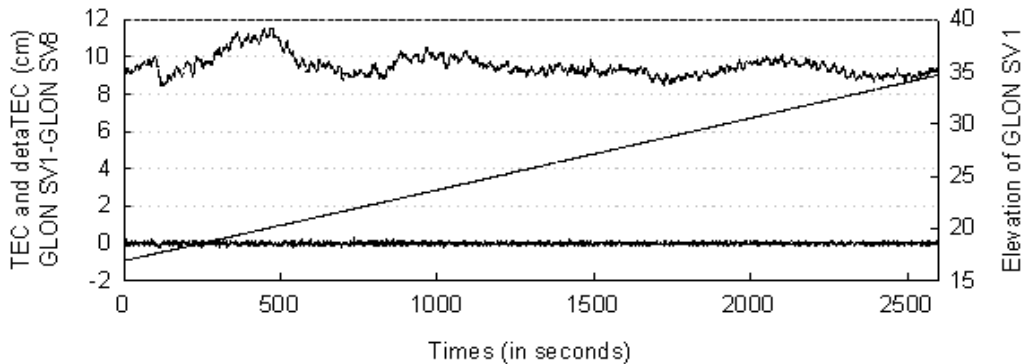


Figure 2. $\nabla\Delta TEC$ and $dTEC$ values for GLONASS Sat 1 (reference GLONASS satellite 8, with highest elevation).

In order to demonstrate the power of the multiple detection procedure based on correlation analysis theory, the 9th epoch in the A1 data containing 5 GPS satellites and 7 GLONASS satellites is analyzed. In this epoch, the ambiguities cannot be fixed correctly. Hence, the previous epoch's fixed ambiguities are introduced. Five (5) simulated outliers are added to the GPS 3 (0.5 cycle), 19 (1 cycle) and 27 (1 cycle)

satellites, and the GLONASS 38 (1 cycle) and 48 (.2 cycle) satellites. Table 4 lists the relevant numerical results of the multiple outlier detection on a step-by-step basis.

Table 4. The test results of multiple outlier detection algorithm with 5 simulated outliers.

Iterations		SV3 (-0.5)	SV 19 (1.0)	SV 27 (1.0)	SV 31	SV 39	SV 40	SV 38 (1.0)	SV 42	SV 48 (0.2)	SV 52	V ^T PV	$r_{R,V}$ (1-0.05)	Upper Boundary $\chi^2(1-0.05)$
1	V	0.63	-0.64	0.13	0.30	0.56	0.76	-0.16	0.83	-0.22	0.40	1386.5	0.549	12.59 FAIL
	R	0.84	1.67	0.18	0.35	1.78	0.94	0.92	0.89	0.24	0.19			
	ρ	0.36	-0.61	-0.22	0.07	0.21	0.32	-0.31	0.40	-0.37	0.12			
2	V	0.85		-0.36	0.55	0.44	0.40	-0.17	0.44	-0.04	0.67	652.09	0.582	11.07 FAIL
	R	1.54		0.66	0.87	1.95	0.68	1.34	0.65	0.07	0.44			
	ρ	0.48		-0.43	0.13	0.28	0.34	-0.59	0.35	-0.46	0.31			
3	V	0.46		-0.57	-0.08	0.05	0.37		0.36	-0.32	-0.12	203.72	0.621	9.49 FAIL
	R	1.46		1.77	0.25	0.69	1.05		0.88	0.80	0.14			
	ρ	0.66		-0.84	-0.02	0.19	0.41		0.42	-0.35	-0.15			
4	V	0.37			-0.13	-0.01	-0.03		-0.07	-0.37	0.01	66.14	0.669	7.82 FAIL
	R	1.85			0.59	0.32	0.17		0.34	1.46	0.01			
	ρ	0.87			-0.28	0.05	0.03		-0.09	-0.76	0.08			
5	V				0.11	-0.03	0.02		-0.02	-0.19	0.13	11.45	0.729	5.99 FAIL
	R				1.31	1.67	0.18		0.22	1.69	0.48			
	ρ				0.33	-0.79	0.33		0.08	-0.96	0.54			
6	V				-0.01	0.00	0.02		-0.02		0.08	0.46	0.805	3.84 5.2 PASS
	R				1.12	0.57	1.03		0.63		1.16			
	ρ				-0.93	-0.90	0.63		-0.12		0.94			
Estimated Outliers		-0.48	1.00	1.11				0.99		0.29				5.3

For each iteration, three sub-rows are included. The first sub-row is the residual value (in cycles), the second sub-row is the standardized residual, and the third sub-row is the correlation coefficient between the residual vector and the column vector of the reliability matrix. The 12th, 13th and 14th columns give the quadratic form of the residuals and the corresponding upper boundary value of the $r_{R,V}$ and the χ^2 -distribution statistic respectively.

From Table 4 it is clearly seen that in the first iteration the maximum residual and standardised residual exists for satellites 42 and 39. However, they have no any artificial outlier actually. It should also be noted that the maximum standardised residual is less than 2. The outliers can not be located through the data snooping and τ test procedures. Fortunately, the outliers can be located through the correlation coefficient test with the application of the iterative process. At each iteration, the satellite containing the biggest outlier will be removed until the χ^2 -distribution test can pass or the maximum $r_{R,V}$ is less than the critical value with the significance level $1-\alpha$ and degrees of freedom $n-2$. At last, the identified outliers values are estimated and given in the last rows. The conclusion can be drawn that the outlier detection procedure based on the correlation analysis theory can indeed locate multiple outliers. It is especially powerful when only one outlier occurs. The applied

algorithm for multiple outlier detection can work well not only for independent observations, but also for highly correlated observations.

5.2 Kinematic Experiment

The second is a kinematic experiment carried out on 29 April 1999 using two GG24 GPS/GLONASS single-frequency receivers and three dual-frequency Leica SR399 GPS receivers. One GG24 receiver and one Leica SR399 were set up at the reference site. The other GG24 receiver and the two Leica GPS receivers were mounted on a car. The trajectory of the rover receivers is shown in Figure 3. (The reason for using three rover receivers is as a mutual check on whether the derived positioning results are correct.) The experiment started on the roadside of the M4 Motorway, Sydney, which is nearby to the reference site. After the first 40 minutes in static mode, the car moved along the Motorway and the Great Western Highway, finishing the experiment in static mode again for 15 minutes. This concluded a single loop. A total of two loops were completed with 1Hz data rate. The number of observed satellites is plotted in Figure 4.

In this kinematic experiment the processed results are shown in Table 5. The constant distance (about 60cm) between the two Leica receivers and one GG24 receiver was used to check whether or not the kinematic positioning results were correct. If distance differences between the Leica rover receivers and the GG24 rover receiver exceeded some specified tolerance value (10cm in this experiment), the ambiguities are considered to have been fixed to the wrong values.

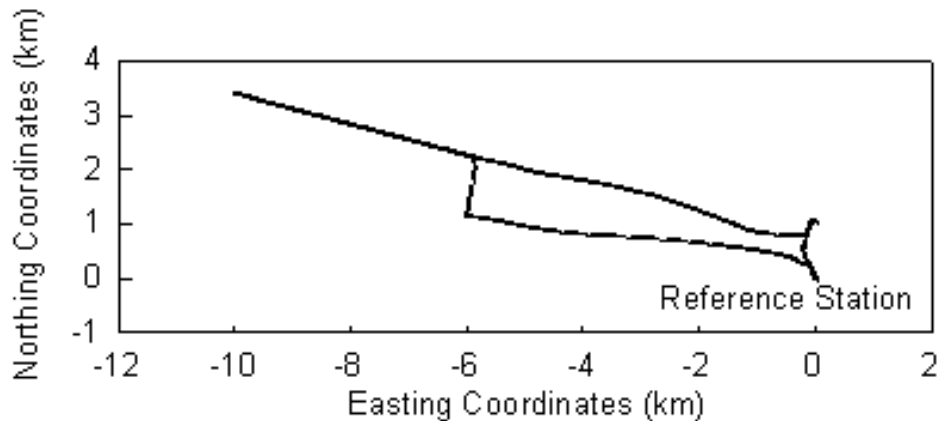


Figure 3. Trajectory of the rover receivers relative to the reference station.

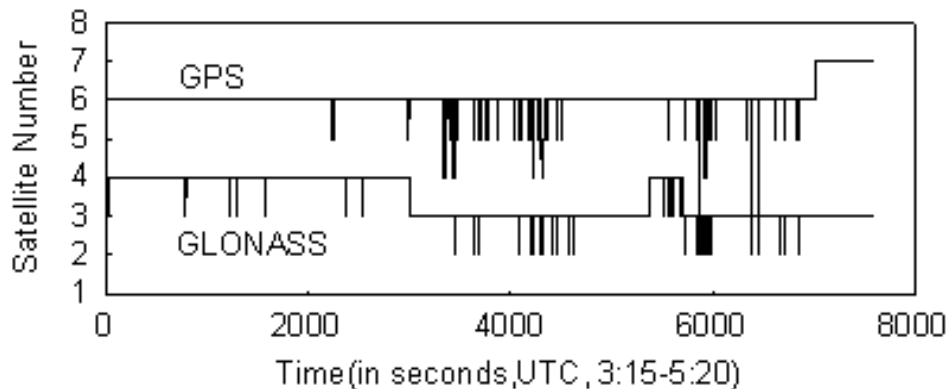


Figure 4. Number of observed satellites in this experiment.

From Table 5 it can be seen that using the elevation-dependent empirical stochastic model the success rate for ambiguity resolution is only 62.4% for the GG24 receivers, and 87.7% and 87.8%

for the Leica receivers. The percentage of rejected epochs is 33%, 12.3% and 12.2% respectively. It also shows that quite a large percentage of epochs (4.6%) in B3 from the GG24 receiver give the wrong ambiguity resolution results.

Table 6 lists the processing results after applying the proposed multiple outlier detection procedure and real-time stochastic model. The success rates of single-epoch ambiguity resolution, or correct positioning results, can be significantly improved to 98.2%, 99.3% and 99.9%. No wrong ambiguity resolution results or incorrect positioning results, estimated by using fixed ambiguities that are introduced from the previous epoch, are accepted. It can also be seen that the multiple outlier detection procedure contributes quite a large percentage of epochs (4.4% for B1, 5.2% for B2, 19.7% for B3) whose ambiguities are fixed correctly or whose positioning results are output correctly. The results indicate that single-epoch ambiguity resolution or correct positioning results can be achieved up to a 99.3% success rate. The results also indicate that the proposed multiple detection procedure has the ability to detect outliers even in correlated observations.

Table 5. kinematic positioning results using a single epoch of data.

Baseline Name	Total Epochs	Correct (%)	Reject (%)	Wrong (%)
B1 Leica 1	5767	5762 (87.8%)	705 (12.2%)	0 (0.0%)
B2 Leica 2	5720	5019 (87.7%)	701 (12.3%)	0 (0.0%)
B3 GG24	7572	4721 (62.4%)	2501 (33.0%)	350 (4.6%)

Table 6. Single-epoch solution using the multiple outlier detection strategy and the real-time stochastic model derived using residuals from previous epochs.

Name	Total Epochs	Correct (%)			Reject (%)	Wrong (%)
		Total	Case 1	Case 2		
B1	5767	5760 (99.9%)	5510 (95.5%)	259 (4.4%)	7 (0.1%)	0 (0.0%)
B2	5720	5682 (99.3%)	5383 (94.1%)	299 (5.2%)	38 (0.7%)	0 (0.0%)
B3	7572	7436 (98.2%)	5945 (78.5%)	1491 (19.7%)	136 (1.8%)	0 (0.0%)

6 CONCLUDING REMARKS

The proposed adaptive procedure has been investigated. The outlier detection algorithm based on correlation analysis can locate rapidly and reliably the outliers or biases even in the case of highly correlated observations. It is especially powerful for only one outlier with a small value and for small degrees of freedom. It can improve significantly the ambiguity resolution success rate and the number of valid kinematic positioning solution epochs. The real-time adaptive stochastic model estimated from the residuals can also significantly improve the ambiguity resolution success rate, and the accuracy of the final solutions.

The results indicate that using the proposed adaptive procedure results in a 99.3% success rate for single-epoch solutions, based on the analysis of four static dual-frequency and single-frequency GPS/GLONASS experiments. The single-epoch solution for kinematic positioning using dual-

frequency GPS-only receivers and single-frequency GPS/GLONASS receivers can achieve up to a 98.3% success rate over 10km baseline lengths.

This algorithm has been designed for real-time applications. Although the data has been post-processed, all computations were carried out in a simulated real-time processing mode.

REFERENCES

- Baarda W. (1968), A testing procedure for use in geodetic networks, Netherlands Geodetic Commission, *Publications on Geodesy*, New Series, Vol.2, No.5.
- Dai L., S. Han & C. Rizos (1999), A multiple outlier detection algorithm for instantaneous ambiguity resolution for carrier phase-based GNSS positioning, *Int. Symp. on Digital Earth (ISDE)*, Beijing, P.R. China, 29 November - 2 December, 321-332.
- Dai L., S. Han & C. Rizos (2001), Performance analysis of integrated GPS/GLONASS carrier phase-based positioning, *Submitted to Journal of Geospatial Information Science*.
- El-Rabbany A.E-S. (1994), The effect of physical correlations on the ambiguity resolution and accuracy estimation in GPS differential positioning, *Ph.D. Dissertation*, Dept. of Geodesy & Geomatics Eng., Tech. Rept. No.170, University of New Brunswick, Canada, 161pp.
- Förstner W. (1983), Reliability and discernability of extended Gauss-Markov models, *DGK, Reihe Heft Nr.98*.
- Han S., L. Dai & C. Rizos (1999), A new data processing strategy for combined GPS/GLONASS carrier phase-based positioning, *12th Int. Tech. Meeting of the Satellite Division of the U.S. Inst. of Navigation GPS ION'99*, Nashville, Tennessee, 14-17 September, 1619-1627.
- Han S. (1997), Quality control issues relating to ambiguity resolution for real-time GPS kinematic positioning, *Journal of Geodesy*, 71(6), 351-361.
- Han S. & C. Rizos (1995), A new method for constructing multi-satellite ambiguity combinations for improved ambiguity resolution, *8th Int. Tech. Meeting of the Satellite Division of the U.S. Inst. of Navigation GPS ION'95*, Palm Springs, California, 12-15 September, 1145-1153.
- Jin X.X. (1995), The change of GPS code accuracy with satellite elevation, *4th Int. Conf. on Differential Satellite Navigation Systems*, Bergen, Norway, 24-28 April.
- Kubik K. (1982), An error theory for the Danish method, Symposium of Comm. III of ISP, Helsinki.
- Kozlov D. (1997), Instant RTK cm with low cost GPS+GLONASS™ C/A receivers, *10th Int. Tech. Meeting of the Satellite Division of the U.S. Inst. of Navigation GPS ION'97*, Kansas City, Missouri, 16-19 September, 1559-1569.
- Leick A. (1998), GLONASS satellite surveying, *Journal of Surv. Eng.*, 121, 91-99.
- Li D. (1988), Error processing and reliability theory, *Press for Surveying and Mapping* (Chinese)
- Pratt M., B. Burke & P. Misra (1998), Single-epoch integer ambiguity resolution with GPS-GLONASS L1-L2 data, *11th Int. Tech. Meeting of the Satellite Division of the U.S. Inst. of*

Navigation GPS ION'98, Nashville, Tennessee, 15-18 September, 389-398.

Rapoport L. (1997), General purpose kinematic/static GPS/GLONASS postprocessing engine, *10th Int. Tech. Meeting of the Satellite Division of the U.S. Inst. of Navigation GPS ION'97*, Kansas City, Missouri, 16-19 September, 1757-1772.

Shi C. (1998), Large scale GPS network adjustment & analysis theory and its application, *Ph.D. Dissertation*, The School of Geoscience and Engineering Surveying, Wuhan Technical University of Surveying and Mapping, 123pp (Chinese).

Teunissen P.J.G. (1994), A new method for fast carrier phase ambiguity estimation, *IEEE Position Location & Navigation Symposium PLANS94*, Las Vegas, Nevada, 11-15 April, 562-573.

Wang J., (1998), Mathematical models for combined GPS and GLONASS positioning, *11th Int. Tech. Meeting of the Satellite Division of the U.S. Inst. of Navigation GPS ION'98*, Nashville, Tennessee, 15-18 September, 899-907.

Wang J. (1999), Stochastic modelling for RTK GPS/GLONASS positioning, *Navigation*, 46(4), 297-305.

Zhodzishsky M., M. Vorobiev, A. Khvalkov & J. Ashjaee (1998), Real-time kinematic (RTK) processing for dual-frequency GPS/GLONASS, *11th Int. Tech. Meeting of the Satellite Division of the U.S. Inst. of Navigation GPS ION'98*, Nashville, Tennessee, 15-18 September, 1325-1331.

Zhou J., Y. Huang, Y. Yang & J. Ou (1997), *Robust Least Square Estimation*, Press. for Huazhong University of Science and Technology (Chinese).